Mechanism for the Plasma Oxidation of Wool Fiber Surfaces from XPS Studies of Self-assembled Monolayers

X. J. DAI,* F. M. ELMS, G. A. GEORGE

Centre for Instrumental and Developmental Chemistry, Queensland University of Technology, GPO Box 2434, Brisbane, Australia

Received 12 November 1999; accepted 17 July 2000

ABSTRACT: The O_2 plasma treatment of self-assembled monolayers (SAMs) of octadecyl mercaptan on gold substrates was investigated as a model for the oxidation of wool fiber surfaces. Three controlled low-pressure gas-plasma treatments were employed in which the active species were (i) atomic oxygen, (ii) atomic oxygen plus vacuum UV radiation, and (iii) full plasma treatment (charged particles in addition to the above). X-ray photoelectron spectroscopy revealed that the plasma treatments differ from each other in the extent of oxidation and etch rate with the full plasma treatment being the most aggressive plasma. The results have confirmed that the charged particles present in a full O_2 plasma treatment are responsible for rapid etching of the organic surface and thus play a significant role in the oxidation mechanism due to radical formation during this process. Vacuum UV radiation also contributes to the oxidation process. Only short plasma treatment is necessary for the oxidation of the lipid layer and the SAM is a suitable model for this process. © 2001 John Wiley & Sons, Inc. J Appl Polym Sci 80: 1461–1469, 2001

INTRODUCTION

The surface of a wool fiber plays a critical role in wool processing, particularly with respect to dye uptake and the adhesion of polymers used for shrinkproofing. The current view[1] of a wool fiber surface is of a protein matrix heavily acylated with lipid, predominantly 18-methyleicosanoic acid [see Fig. 1(a)]. The lipid is attached to the keratin layer via a thioester linkage and the lipid molecules are oriented in the lowest-energy conformation directed away from the surface. Removal of the lipid layer results in improvement in polymer adhesion and dye uptake. The covalently bound lipid can be removed from the fiber surface using a range of chemical means including alkali, chlorine, and amine treatments. The extent of lipid removal is uncertain and varies with the treatment process. Another drawback to chemical processing is that the integrity of the underlying wool fiber can be modified, resulting in degradation of the mechanical properties of the wool and yellowing. These effects are dependent on the severity of the treatment and exposure time.

An alternative to using chemical treatments is to expose the wool fibers to the reactive species generated in a low-pressure gas plasma. A number of studies on the plasma treatment of wool fabric, using oxygen or air as the plasma gas, have been performed.[2,3] The results indicate that plasma-modified wool fabric exhibits enhanced colorfastness, abrasion resistance, tensile strength, and antifelting compared with fabric that has been chlorinated.[2] Plasma treatment of wool fibers results in an increase in surface energy, determined from contact angle measurements, and changes in the chem-

Correspondence to: G. A. George.
* *Present address:* CSIRO Textile and Fibre Technology, Belmont, Victoria, Australia.

Journal of Applied Polymer Science, Vol. 80, 1461–1469 (2001)

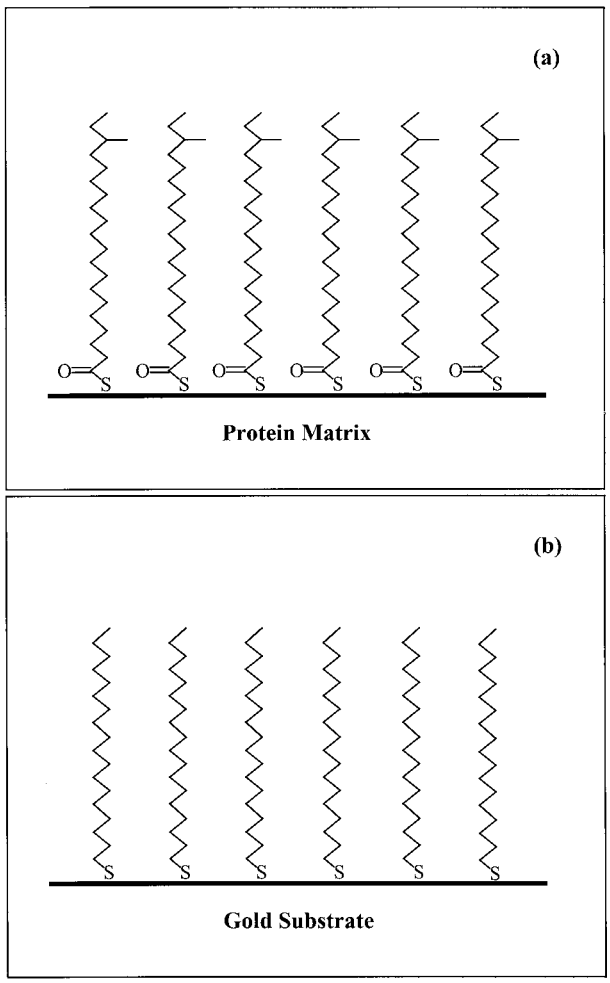

Figure 1 Schematic diagram of the structure of (a) the epicuticle of a wool fiber and (b) and *n*-alkane mercaptan SAM on gold. Note that the alkyl chain tilt of ~ 30° to the surface normal is not shown for the ODM SAM and that the sulfur atoms are covalently bound to the substrates.

ical composition of the surface, as indicated by surface analysis using X-ray photoelectron spectroscopy.[3] A detailed study of the action of oxygen plasma constituents, namely, atomic oxygen [$O(^1S)$], metastable (singlet $^1\Delta_g$) excited molecular oxygen, and charged particles such as O^{2+}, O^{2-}, O^+, O^-, and e^-, concluded that the chemical modification of the wool fiber surface results predominantly by reaction with atomic oxygen and that charged particles play no significant role.[3] No information on the changes that occur in the structure of the wool fiber surface during plasma treatment was afforded by these studies. As a result, no conclusions regarding the extent of lipid removal and the integrity of the underlying wool fiber could be made.

A greater understanding of $O(^1S)$ and plasma effects can be achieved by simplifying the system and studying model surfaces with a well-defined chemical structure and morphology. The surface of wool fibers, although well investigated, are complex, making characterization of surface structures difficult. Organic monolayer films on smooth planar substrates offer a level of structural control that fulfills many of the requirements for model surfaces. Self-assembled monolayers (SAMs) of ω-substituted long-chain *n*-alkane mercaptans on gold substrates are distinguished by their easy synthesis, their stability in both vacuum and ambient environments, and the ability to manipulate the structure and chemical properties of these materials.[4,5]

SAMs are readily formed by immersing the substrate into a solution of the desired adsorbate. The structure of SAMs of *n*-alkane mercaptans on gold has been well characterized using reflection–absorption infrared spectroscopy (RAIR), scanning tunneling microscopy (STM), and electron diffraction studies.[4] The monolayer is a crystalline $(\sqrt{3} \times \sqrt{3})R30°$ overlayer commensurate with the underlying gold lattice. The sulfur atom spacing is 4.97 Å, resulting in a calculated area per molecule of 21.4 Å^2. The molecules exist in an all-*trans* conformation, tilted ~ 30° from the surface normal, 14° away from the nearest-neighbor direction, and are rotated 55° about the chain axis. Thus, SAMs exhibit smooth, homogeneous, low-energy surfaces,[4] ideal for studying reactive modification treatments, such as a low-pressure gas plasma, on organic surfaces.

The structure of SAMs of octadecyl mercaptan (ODM) on gold is not unlike the proposed structure of the surface lipid layer of a wool fiber (see Fig. 1). It is likely that the lipid on the wool fiber surface is also tilted with respect to the substrate (keratin matrix) in order to minimize the conformational interaction energy. The obvious simplification, removal of the branching methyl group and the thioester functionality, does not rule out the use of such monolayers as a model for the lipid layer of the wool fiber surface. Indeed, the use of this simple model allows quantitation of atom–substrate reactions. ODM SAMs have been used to model oxygen effects on polymers such as polyethylene.[6] In this article, the surface modification of self-assembled monolayers of ODM by a controlled oxygen rf low-pressure gas plasma was studied using XPS to relate the various plasma constituents to surface changes. The implications of these results for the plasma treatment of wool fibers is discussed.

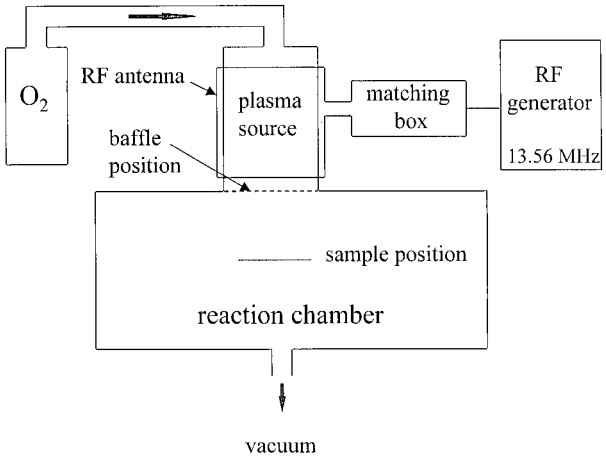

Figure 2 Schematic diagram of the plasma apparatus.

EXPERIMENTAL

Sample Preparation

ODM was purchased from Aldrich (Milwaukee, WI) and used as received. Gold substrates were prepared by evaporation of ~ 2000 Å of gold onto 12-mm^2 pieces of glass microscope slides which had been cleaned in hot H_2SO_4/H_2O_2 (4 : 1) for 15 min, rinsed in deionized water and ethanol, dried in a stream of N_2, and precoated with ~ 50 Å of chromium. The SAMs were prepared by immersing the fresh substrates into 1 m*M* ethanol solutions of the adsorbate.[7]

Gas Plasma Treatments

The plasma apparatus and the density measurements of the plasma constituents (charged and neutral particles) were described in detail elsewhere.[3] Briefly, the plasma constituents, generated at the source, diffuse into the reaction chamber (see Fig. 2). Baffles can be inserted between the source and the reaction chamber to control the flow of various plasma constituents. In the first modification, stainless-steel mesh, with a diameter of 30 μm (well below the local Debye distance of ~ 200 μm of the plasma) was used to reduce the density of charged particles in the reaction chamber without seriously affecting the flux of neutral particles. In the second modification, a loose-fitting glass plate was used in conjunction with the mesh to block both the flux of charged particles and vacuum UV radiation into the reaction chamber. Gas (O_2) was admitted into the plasma chamber to a static pressure between 10^{-3} and 10^{-1} mbar. The plasma was operated at a power level between 25 and 100 W. Treatment times ranged from 1 to 90 s. After plasma treatment, the samples were left in the flowing gas for 3 min before the chamber was evacuated and air admitted. The atomic oxygen concentration multiplied by the exposure time, N[O]t, is used to describe the plasma dose.[3]

Surface Analysis

XPS experiments were carried out in an ultrahigh vacuum using a Physical Electronics Industries PHI Model 560 surface analysis system. This system employs a double-pass cylindrical mass analyzer (20-270AR) with a perpendicularly mounted dual (Mg/Mg) X-ray source. A single MgKα X-ray source was operated at 400 W and 15 kV. The maximum energy resolution of the CMA was 1.2 eV operated for XPS analysis in the fixed analyzer transmission (FAT) mode with a pass energy of 25 eV for the Ag $3d_{5/2}$ emission. The electron binding energies (E_B) were calibrated against the Au $4f_{7/2}$ emission at E_B = 84 eV.[8,9] Samples were mounted on carbon black to limit charging. Typical pressures during analysis were between 5×10^{-8} and 5×10^{-7} Torr. Survey spectra were obtained over the range 0–1000 eV, using a pass energy of 100 eV with an acquisition time of 2 min. Atomic concentrations were quantified using peak areas from 50 eV multiplex spectra (acquisition time 5 min) and experimentally derived elemental sensitivity factors.[10] Sample charging was corrected by referencing binding energies to the Au $4f_{7/2}$ photoelectron peak. High-resolution spectra were obtained at a pass energy of 25 eV for 5 min. Carbon 1s photoelectron peaks were fitted with a least-squares routine using Gaussian/Lorentzian peak shapes. The appropriate constraints for line shape (85% Gaussian/15% Lorentzian) and fwhm were determined by analyzing chemically equivalent standards (polyethylene) under similar data-acquisition conditions.

RESULTS AND DISCUSSION

Characterization of ODM SAMs

Self-assembled monolayers of ODM on gold have been well characterized using XPS.[6] As a consequence, only the salient features of their spectra will be mentioned here. The principal photoelectron peaks for an ODM SAM on gold are the C 1s

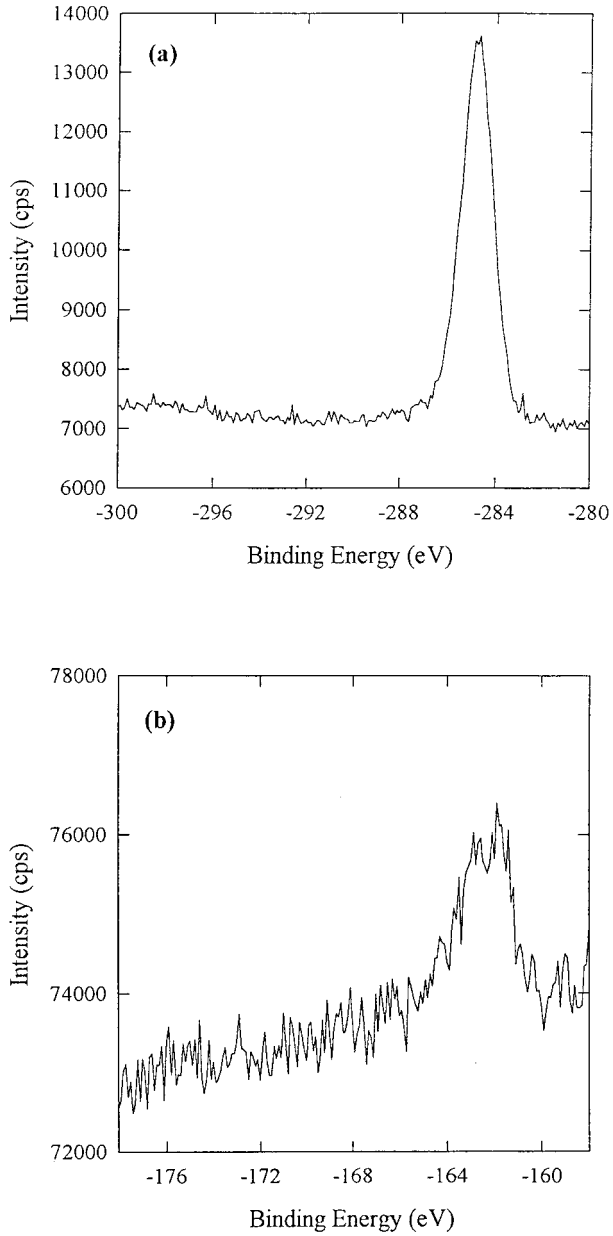

Figure 3 (a) C 1*s* photoelectron peak and (b) S 2*p* photoelectron peak for an ODM SAM on a gold substrate.

and S 2*p* peaks, as shown in Figure 3. A symmetric C 1*s* photoelectron peak, occurring at the binding energy, E_B = 284.6 eV, is consistent with the adsorption of the long-chain aliphatic thiol on the gold surface. The slight tail toward higher binding energy of the C 1*s* photoelectron peak can be attributed to carbon bound to sulfur atoms (C—S) and traces of oxidized carbon contaminants irreversibly adsorbed to the Au substrate. A single, weak S 2*p* photoelectron peak occurring at E_B = 162 eV is consistent with the formation of a thiolate. The relative atomic concentrations for an ODM SAM from ethanol are typically C, 74.0%; Au, 22.4%; S, 2.1%; and O, 1.5%. Decomposition of ODM SAMs occurs at a high X-ray flux (400 W).[6] Also, plasma treatment of hydrocarbon polymers such as polyethylene produces oxygen species on the surface which have been shown to be X-ray sensitive.[11] As similar species may be formed in ODM SAMs, short XPS acquisition times were used to minimize the possible effects of X-ray damage. This reduces the signal-to-noise ratio of the spectra.

Controlled Oxygen Plasma Effects on ODM SAMs

Initial plasma treatment of ODM SAMs was performed without using any baffles between the plasma source and the reaction chamber. As a result, the monolayers were exposed to the full complement of plasma constituents including $O(^1S)$, metastable O_2 ($^1\Delta_a$), O^{2+}, O^{2-}, O^+, O^-, e^-, and vacuum UV radiation. Figure 4 shows the variation in relative atomic concentration of C and O for an ODM SAM as a function of the plasma dose. The O 1*s*/C 1*s* photoelectron peak intensity ratio increased rapidly with the plasma dose, reaching a steady value of 0.64 at plasma doses greater than 13×10^{13} cm^{-3} s. The full O_2 plasma treatment resulted in rapid oxidation of

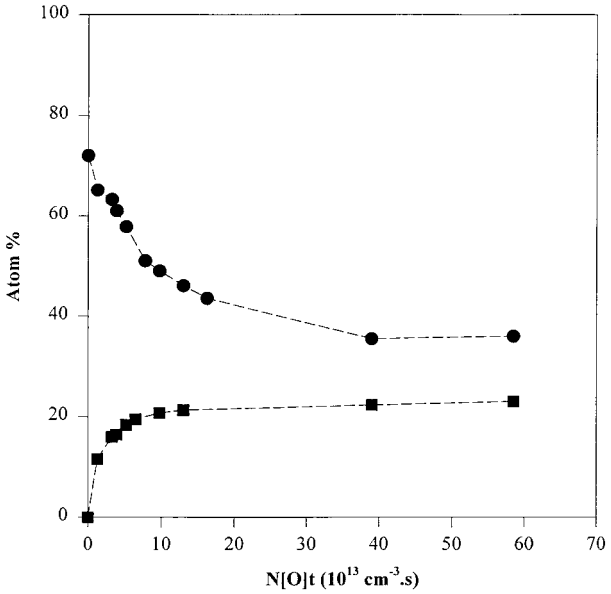

Figure 4 Variation in the relative concentration of (●) C and (◆) O for an ODM SAM following full O_2 plasma treatment.

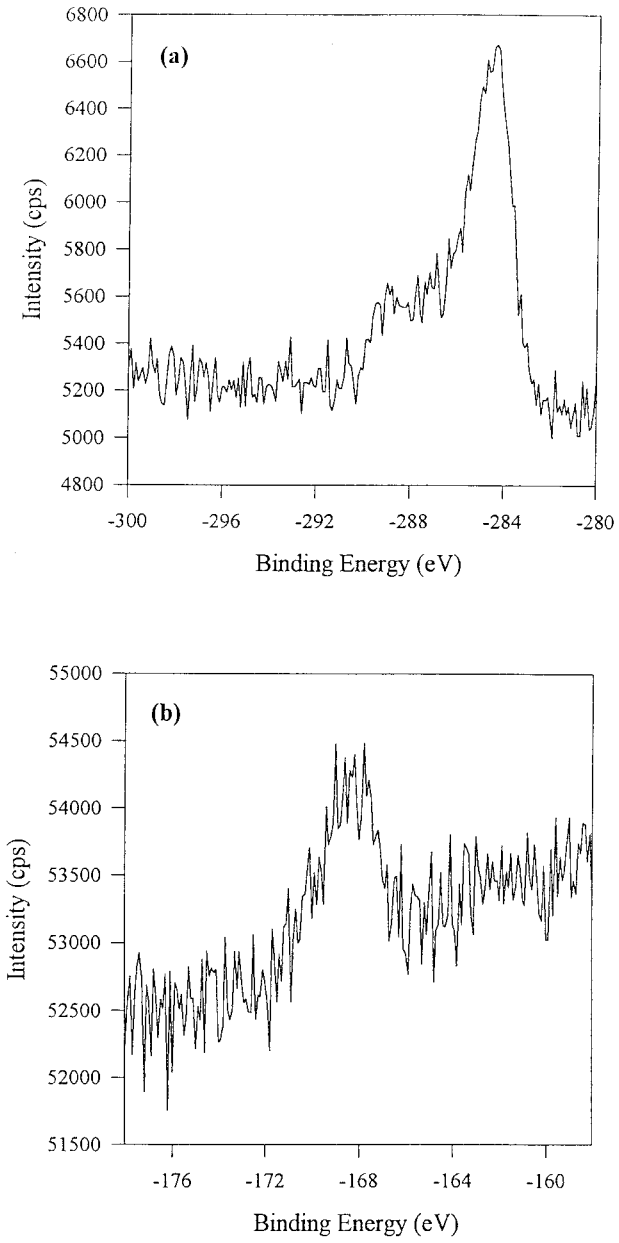

Figure 5 (a) C 1*s* photoelectron peak and (b) S 2*p* photoelectron peak for an ODM SAM on a gold substrate exposed to a full O_2 plasma treatment at N[O]t = 13 × 10^{13} cm^{-3} s.

the monolayer. XPS results showed a dramatic loss of carbon from the surface, indicating etching of the SAM.

The principal photoelectron peaks (C 1*s* and S 2*p*) for an ODM SAM treated with a plasma dose N[O]t = 13 × 10^{13} cm^{-3} s are shown in Figure 5 and may be contrasted with those from the original material (Fig. 3). The C 1*s* photoelectron peak [Fig. 5(a)] is now broad and asymmetric with a tail to higher binding energy consistent with a range of oxidized species.[12] The single S 2*p* photoelectron peak [Fig. 5(b)] occurring at a higher binding energy, E_B = 168.2 eV, is consistent with oxidation of the sulfur headgroup and the formation of sulfonate (RSO_3) species.[12] Formation of the sulfonate species, indicated by the appearance of the oxidized-sulfur S 2*p* photoelectron peak (E_B = 168.2 eV), was observed after a plasma dose N[O]t = 6.5 × 10^{13} cm^{-3} s and complete oxidation of the ODM sulfur atom was observed at N[O]t = 13 × 10^{13} cm^{-3} s. Increase in the O content after this dose does not involve contribution from the S—O species. Oxidation of the substrate may be recognized by a broadening of the Au $4f_{7/2}$ photoelectron peak; a shift of 0.4 eV to higher binding energy is expected for the formation of the Au—O species.[13] Oxidation of the Au substrate was observed by XPS after a plasma dose N[O]t = 39 × 10^{13} cm^{-3} s. These results indicate that carbon oxidation and C—C bond scission occur prior to any oxidative processes at the Au—S interface.

The remaining plasma treatment of ODM SAMs was performed using baffles between the plasma source and the reaction chamber. Fine stainless-steel mesh was used to stop charged particles from entering the reaction chamber without significantly reducing the concentration of neutral particles in the chamber, while glass, in addition to the mesh, was used to block vacuum UV radiation impinging on the sample surface. Figure 6 shows the variation in relative atomic concentration of C and O as a function of plasma dose for both plasma baffles (mesh and mesh + glass). For both baffles, the XPS results show a much slower rate and lower extent of oxidation of the surface, compared with the full plasma treatment (Fig. 4), with a maximum O 1*s*/C 1*s* ratio of 0.35 achieved at the completion of treatment. Formation of sulfonate species, indicated by the appearance of the oxidized-sulfur S 2*p* photoelectron peak (E_B eV), was not observed until a plasma dose N[O]t = 24 × 10^{13} cm^{-3} s. Complete oxidation of the ODM sulfur atom was not observed. No oxidation of the Au substrate was observed by XPS even after a plasma dose N[O]t = 180 × 10^{13} cm^{-3} s. Comparison of the XPS results for the two plasma treatment conditions (Fig. 6) shows a difference in the rate of oxidation for doses lower than 20 × 10^{13} cm^{-3} s (see Fig. 6). In more specific terms, the relative increase in oxygen on the surface, concomitant with the loss of carbon, is faster when mesh alone is used as the

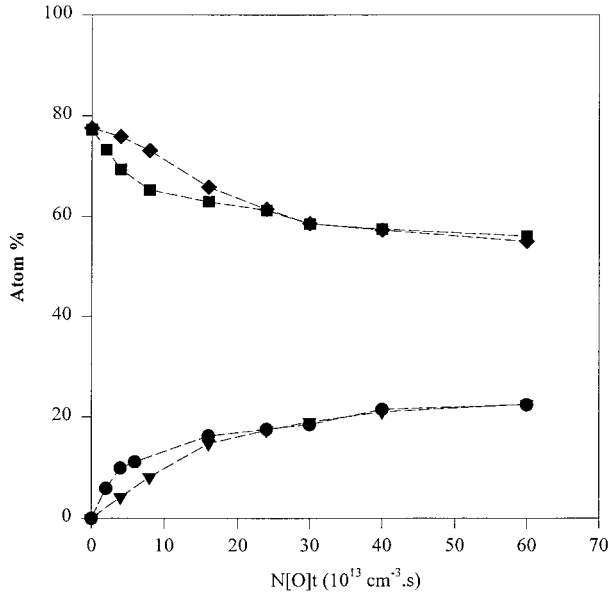

Figure 6 Variation in the relative concentration of C and O for an ODM SAM following O_2 plasma treatment using baffles; mesh: (◆) C, (●) O; mesh + glass: (■) C, (▼) O.

baffle. In this case, the SAM is exposed to the vacuum UV radiation generated by the plasma. These results indicate that vacuum UV radiation significantly contributes to the oxidation process.

The function of the various plasma constituents can be determined by comparing the XPS results for each plasma case (namely, in the absence or presence of baffles). Figure 7 shows the variation in the atomic concentration of gold (the SAM substrate) for an ODM SAM as a function of plasma dose. A rapid rise in the relative concentration of gold (Fig. 7) on the surface which was exposed to the full plasma treatment (no baffles), concomitant with the rapid decrease in the carbon concentration (Fig. 4), is clearly observed. The increase in surface oxygen content (Fig. 4), although confined to oxidation of the long aliphatic carbon chains of the ODM molecules at a low plasma dose, can be attributed to oxidation at the Au—S interface for plasma doses higher than 6×10^{13} cm^{-3} s. These results are consistent with etching (*complete removal*) of the SAM from the substrate. This trend is not reproduced for the other plasma treatments where baffles prevent the transport of charged particles into the reaction chamber. For these plasma treatments, no significant increase in the surface Au concentration is observed and only partial oxidation of the sulfur headgroup is achieved. Thus, charged particles are responsible for the etching of organic surfaces.

Information about the plasma oxidation of an organic surface is available by careful study of the C 1*s* photoelectron peak. Figure 8(a–c) shows the curvefitted C 1*s* photoelectron peaks for ODM SAMs treated by the three O_2 plasmas, respectively, at a plasma dose $N[O]t = 8 \times 10^{13}$ cm^{-3} s. For each case, the C 1*s* photoelectron peak is asymmetric with a tail to higher binding energy consistent with a range of oxidized species.[12] Comparison of the three C 1*s* photoelectron peaks shows distinct differences in the shapes of the higher binding energy tail. The relative concentrations of the oxidized species were determined using a curve-fitting protocol with fixed line shapes and band positions and the results are given in Table I. It is evident that a full O_2 plasma treatment results in a higher proportion of oxidized species (concomitant with a higher total oxygen concentration). Comparison of the species distributions show a difference in the relative concentrations of the functional groups for all the plasma treatments. The higher concentration of the more oxidized species (C═O, O—C—O, O—C═O) achieved by the full O_2 plasma treatment indicates a difference in the mechanism of oxidation rather than just a difference in the oxidation rate. In the presence of all plasma constituents, oxidation of

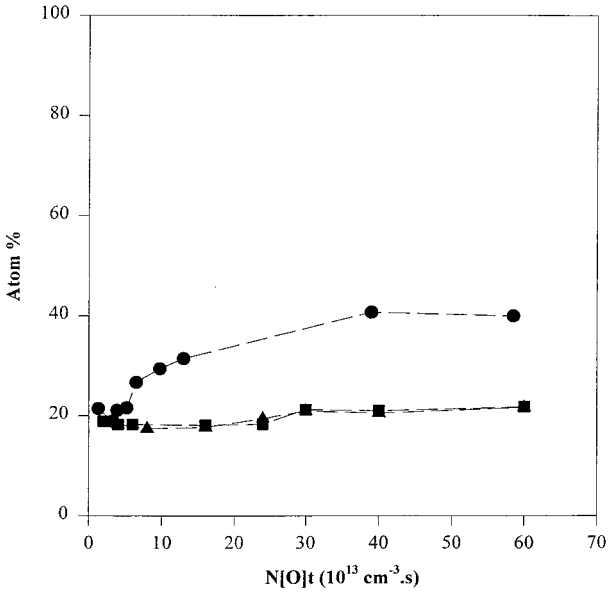

Figure 7 Variation in the relative concentration of Au for and ODM SAM following O_2 plasma treatments: (●) no baffles; (■) mesh; (▲) mesh + glass.

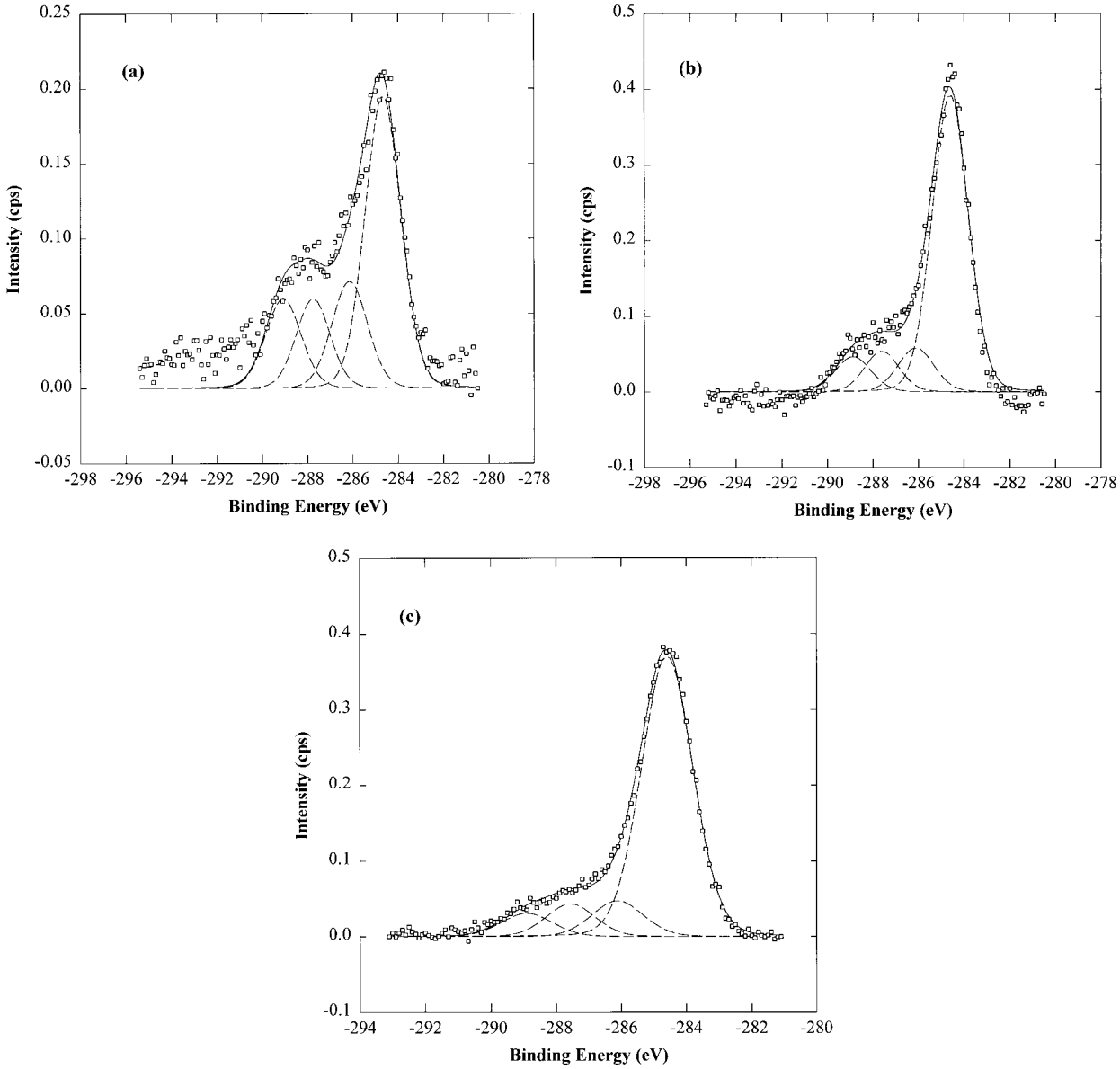

Figure 8 C 1*s* photoelectron peak for an ODM SAM following O_2 plasma treatment at $N[O]t = 8 \times 10^{13}$ cm^{-3} s: (a) no baffles; (b) mesh; (c) mesh + glass.

the surface is enhanced because molecular oxygen, present in the chamber, can react with radicals formed during the etching process. The low concentration of oxidized species for the O_2 plasma baffled with mesh and glass relative to those for the plasma baffled with mesh alone indicates that vacuum UV radiation also contributes to the oxidation mechanism.

Implications for Plasma Treatment of Wool Fibers

The O_2 plasma treatment of wool fabric as an alternative to using chemical treatments was investigated[2,3] and the results showed that plasma-modified wool fabric exhibits enhanced colorfastness, abrasion resistance, tensile strength, and antifelting compared with fabric that has been chlorinated.[2] No information on the changes that occur in the structure of the wool fiber surface during plasma treatment was afforded by these earlier studies. As a result, no conclusions regarding the extent of lipid removal and the integrity of the underlying keratin matrix were made. The similarity between the structure of an ODM SAM and a wool fiber surface (Fig. 1) allows the use of

Table I Relative Concentration of Surface Functional Groups After Plasma Treatment, N[O]t = 8 × 10^{13} cm^{-3} s, as Determined by Curve-fitting the C1s Photoelectron Peak of an ODM SAM

Species E_B (eV)	C—C 284.6	C—O 286.1	C═O; O—C—O 287.6	O—C═O 288.8
Full O_2 Plasma	50.8	18.6	14.8	15.6
Mesh O_2 plasma	71.5	10.6	9.4	8.5
Mesh + glass O_2 plasma	75.5	9.7	8.5	6.3

ODM SAMs to model the effects of light O_2 plasma treatment on wool fibers.

On the basis of the above results, a number of conclusions about the structural changes in the lipid layer of a wool fiber surface following O_2 plasma treatment can be drawn: Treatment of wool fibers using a full O_2 plasma would result in rapid and complete removal of the lipid layer. Removal of the lipid layer results in improvement in dye uptake and polymer adhesion which is important for colorfastness and shrinkproofing. This result would be obtained using very short treatment times (N[O]t < 6 × 10^{13} cm^{-3} s). Prolonged plasma treatment would result in oxidation of the underlying keratin matrix, which could lead to degradation of the mechanical properties of the wool fibers. The SAM studies cannot provide information about this process. Controlled plasma oxidation for short times, where the major reactive species is atomic oxygen, would result in oxidation of the lipid layer alone. In this case, the hydrophobic lipid layer has been rendered polar and the formation of reaction sites has occurred. This should allow for improved dye uptake and polymer adhesion. The added advantage of using a less vigorous O_2 plasma is that the integrity of the underlying keratin matrix would be maintained, ruling out any degradation of the mechanical properties of the wool fiber. Recent studies[14] of the treatment of wool fibers using this controlled O_2 plasma have supported the above conclusions with the results that complete oxidation of the surface at a low plasma dose corresponds to maximum improvement in printing and shrinkage, while maximum improvement in dye uptake occurs when the lipid layer is removed by etching at a high plasma dose.

CONCLUSIONS

The action of a low-pressure O_2 plasma on an organic surface involves two processes: surface etching and surface oxidation. The influence of the various plasma constituents on these two mechanisms have been clearly illustrated by this study. The charged particles present in a full O_2 plasma treatment have been shown to be responsible for rapid etching of the organic surface and thus play a significant role in the oxidation mechanism due to radical formation during this process. Vacuum UV radiation also contributes to the oxidation process. By using an ODM SAM as a simple model of a wool fiber surface, it can be concluded that the treatment of a wool fiber using a full O_2 plasma would result in rapid and complete removal of the lipid layer and oxidation of the underlying keratin matrix, thereby enhancing dye uptake and polymer adhesion. Controlled plasma oxidation, using less vigorous O_2 gas plasma treatments, would result in oxidation of the lipid layer alone. This may allow for improved dye uptake and polymer adhesion, due to the formation of reaction sites on a hydrophobic surface which has been rendered polar, with the added advantage of maintaining the integrity of the underlying keratin matrix.

REFERENCES

1. Negri, A. P.; Cornell, H. J.; Rivett, D. E. Text Res J 1993, 63, 109.
2. Rakowski, W. Melliand Text 1989, 70, 780.
3. Dai, X. J.; Hamberger, S. M.; Bean, R. A. Aust J Phys 1995, 48, 939.

4. Dubois, L. H.; Nuzzo, R. G. Annu Rev Phys Chem 1992, 43, 437.
5. Ulman, A. Chemtech 1995, 3, 22.
6. Elms, F. M.; George, G. A. Polym Adv Technol 1998, 9, 31.
7. Bain, C. D.; Troughton, E. B.; Tao, Y.-T.; Evall, J.; Whitesides, G. M.; Nuzzo, R. G. J Am Chem Soc 1989, 111, 321.
8. Bird, R. J.; Swift, T. J Electron Spectrosc Relat Phenom 1980, 21, 227.
9. Seah, M. P. Surf Interface Anal 1989, 14, 488.
10. Ward, R. J.; Wood, B. J. Surf Interf Anal 1992, 18, 679.
11. Chappell, P. J. C.; Brown, J. R.; George, G. A.; Willis, H. A. Surf Interf Anal 1991, 17, 143.
12. Handbook of X-ray Photoelectron Spectroscopy; Perkin–Elmer Corp. Physical Electronics Division: Eden Prairie, MN, 1979.
13. Ron, H.; Rubinstein, I. Langmuir 1994, 10, 4566.
14. Bean, R. A.; Holcombe, B. V.; Turner, P. S.; Dai, X. J.; Hamberger, S. M. Text Res J, in press.